WOOLPERT

ARCHITECTURE | ENGINEERING | GEOSPATIAL

PI CNMI 2019 D19

Lidar Mapping Report
Project ID - 175072
Work Unit - 211535

USGS CONTRACT NUMBER: G16PC00022

TASK ORDER: 140G0219F0063

NOAA CONTRACT NUMBER: EA-133C-16-CQ-0046

November 15, 2021

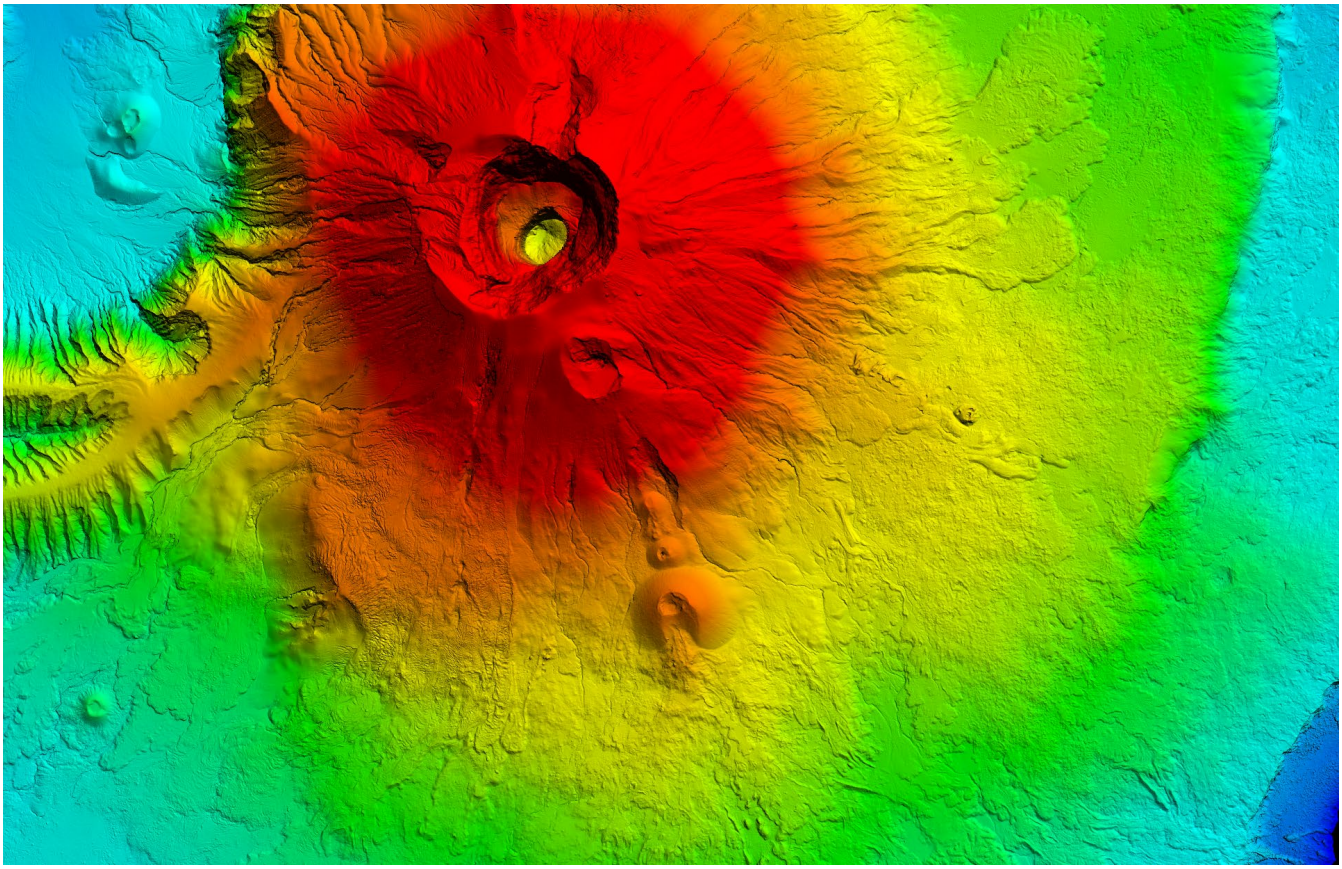

TABLE OF CONTENTS

1. EXECUTIVE SUMMARY 3

1.1. Survey Area 3

2. DATA ACQUISITION 4

2.1. Mobilization 4

2.1.1. Aircraft Offset Survey 5

2.2. Lidar Calibration 5

2.3. Aerial Survey Operations 8

2.3.1. The Hawkeye 4X Sensor 10

2.3.2. Positioning 12

2.3.3. PPP Shifts 12

2.4. Ground Survey Operations 13

2.4.1. Primary Control Points 13

2.4.2. Lidar Ground Survey Points (GSPs) 13

2.4.3. Lidar Ground Check Points (GCPs) 13

3. DATA PROCESSING 13

3.1. Position 14

3.2. Lidar 15

3.2.1. Raw Data Processing 15

3.2.2. Lidar Data Editing 16

3.3. Reflectance 17

4. QUALITY CONTROL 18

4.1. Calibration 18

4.2. Online Checks 18

4.3. Positioning 18

4.4. Topo Comparison to Adjacent Lines 18

4.5. Bathy Crossline Analysis 18

4.6. Absolute Vertical Accuracy Checks 19

5. DELIVERABLES 19

5.1. Classified Point Cloud (LAS Files) 20

APPENDIX A : FLIGHT LOGS 21

APPENDIX B : PROCESSING LOGS 22

Table 1: Survey Areas 4
Table 2: Aircraft Offsets 5
Table 3: August 25, 2019 Calibration QA Results 7
Table 4: February 23, 2020 Calibration QA Results 7
Table 5: July 14, 2020 Calibration QA Results 7
Table 6: August 25, 2019 Calibration Ground Truth Comparisons 7
Table 7: February 23, 2020 Calibration Ground Truth Comparisons 7
Table 8: July 14, 2020 Calibration Ground Truth Comparisons 8
Table 9: Summary of Daily Operations 8
Table 10: Survey Flight Parameters 11
Table 11: GNSS Base Stations Used for Trajectory Processing, NAD83 (MA11) Epoch 2010.0 12
Table 12: Corrections for PPP Shift 12
Table 13: Inertial Explorer Offsets 14
Table 14: Overlap Consistency 18
Table 15: Cross Line Point to Surface Results 19
Table 16: Crossline Surface Difference Results 19
Table 17: Project Datum and Projection 19
Table 18: Lidar Product Deliverables 19
Table 19: Delivered LAS Classes 20

Figure 1: Planned Topo-Bathy (Hawkeye 4X) Survey Area 4
Figure 2: Mobilized Survey Aircraft 5
Figure 3: Schematic of HE3 Calibration Lines 6
Figure 4: Hawkeye 4X Bathymetric Lidar Sensor Installation 11
Figure 5: Overview of Processing Workflow 14
Figure 6: Sample Waveform in Shallow Water 15
Figure 7: Sample LSS Processing Screen 16

1. EXECUTIVE SUMMARY

Woolpert Inc. (Woolpert) was contracted for a two-part lidar data acquisition and lidar data processing effort in the Commonwealth of the Northern Mariana Islands. Part one required lidar data acquisition, initial data processing, and data coverage verification in the field performed under the United States Geological Survey (USGS) Contract G16PC00022, Task Order Number 140G0219F0063 (USGS PI NMCI 2019 D19). Part two is for the final data processing, derivative lidar products, and QA/QC and is performed under the NOAA Office of Coastal Management (NOAA) Contract EA-133C-16-CQ-0046, Order Number 1305M219FNCNP0087 (T-0087-CNMI Lidar).

Woolpert collected lidar using their Hawkeye 4X topo-bathy lidar sensor, to provide high density topographic lidar to meet National Geospatial Program Lidar Base Specification Version 1.3 QL1 standard, while simultaneously acquiring bathymetric lidar data at National Coastal Mapping Strategy 1.0 QL2b standard.

Details of the survey, data processing, QC and product creation are provided within this report.

1.1. SURVEY AREA

The project included six areas of interest to be surveyed with topo-bathy lidar, identified as the islands of Pagan, Farallon de Medinilla, Saipan, and Tinian, Aguijan, and Rota. Survey areas are provided in Table 1 below, and shown in Figure 1. The islands of Saipan, Tinian, Aguijan, and Rota fall within Work Unit 211535. This work unit was delivered with the following Coordinate Reference System (CRS):

Horizontal Datum	NAD83 (MA11) Epoch 2010.0
Vertical Datum	NMVD03 (Geoid 12B), Orthometric Heights
Projection	UTM 55N
Units (Horizontal and Vertical)	Meters

Woolpert conducted a simultaneous collect of topographic and bathymetric lidar using its Leica Hawkeye 4X sensor. All topo lidar data were collected to meet United States Geological Survey Quality Level 1 (USGS QL1) and all bathymetric lidar data were collected to meet accuracy requirement for the National Coastal Mapping Strategy v.10 Quality Level 2b (QL2b).

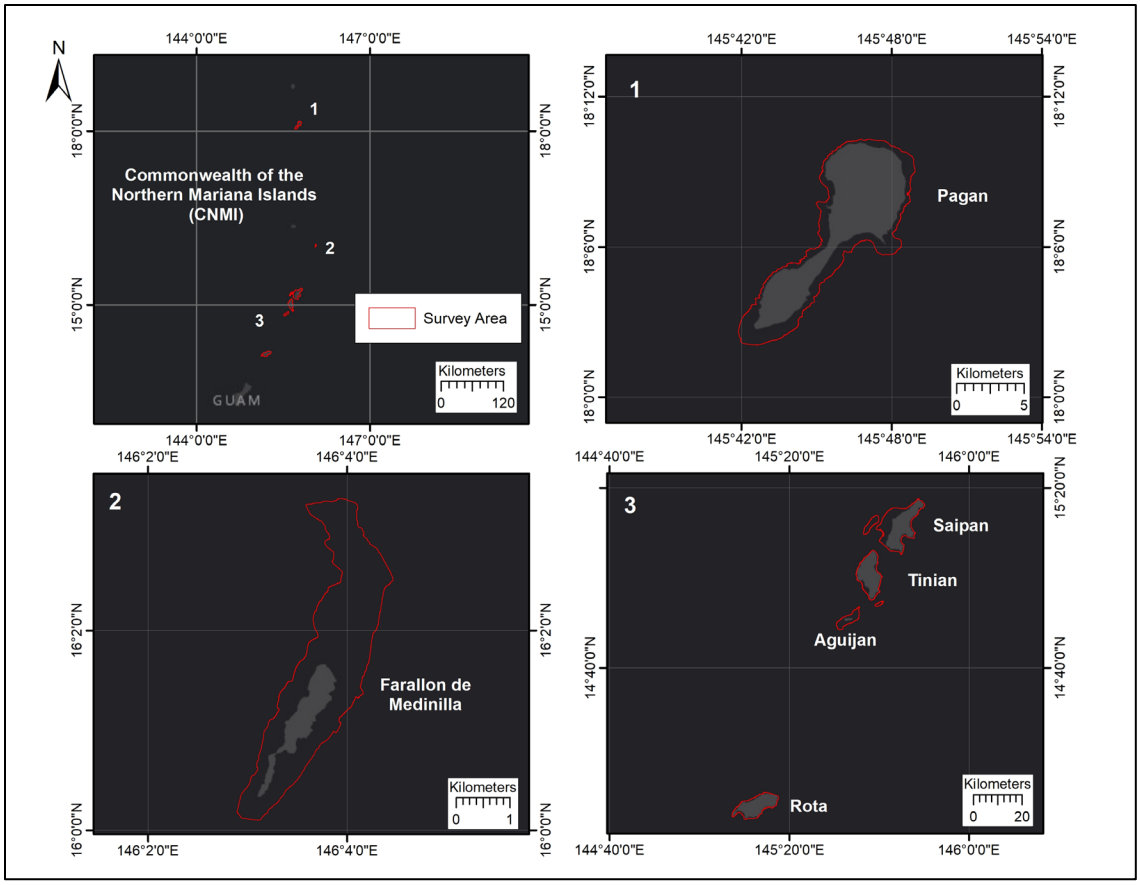

Figure 1: Planned Topo-Bathy (Hawkeye 4X) Survey Area

Table 1: Survey Areas

Location	Planned Survey Area (square kilometers/square miles)
Pagan	71/27
Farallon de Medinilla	6/2
Saipan	227/88
Tinian	129/50
Aguijan	35/14
Rota	109/42

2. DATA ACQUISITION

All lidar data were acquired using a Hawkeye 4X (HE4X) sensor. The HE4X sensor was mounted in a Leica PAV100 gyro-stabilized mount integrated with a NovAtel SPAN GNSS and LCI-100C IMU. Real time navigation and GNSS/IMU data logging was provided by Leica FlightPro software. Lidar data were logged on the Airborne Hydrography, AB (AHAB) operator console.

Below are the details of the lidar collection and processing.

2.1. MOBILIZATION

The HE4X was installed in a Reims-Cessna 406 (ZK-XLF) owned and operated by Kiwi Air. Calibration flights were collected over Saipan on August 25, 2019, February 23, 2020, and July 14, 2020. Survey data were acquired from

July 5 to August 25, 2019, February 12 to February 26, 2020, and June 19 to July 14, 2020. There was 1 aircraft maintenance day during the first collect in 2019.

Figure 2: Mobilized Survey Aircraft

2.1.1. Aircraft Offset Survey

Physical mounting offsets between the GNSS antenna, IMU and gyro-stabilized mount were determined through a combination of manual measurements and iterative processing in NovAtel Inertial Explorer software.

Manual measurements were taken from the GNSS antenna to the reference point on the IMU in the HE4X sensor head. These measurements are added to the known offset between the IMU reference point and the rotation center of the gyro-stabilized mount to calculate the preliminary offset between the GNSS antenna and sensor reference point. This preliminary value was then used to seed the post-processing software which, through an iterative computation, uses the dynamic accelerations and rotations during flight to refine the offsets. Once the solution converges, the final offsets are entered into the flight management software and used in subsequent post-processing of the GNSS/IMU data for final trajectories.

Final offsets, shown in the Leica reference frame, are presented in Table 2.

Table 2: Aircraft Offsets

Sensor Head	Lever Arm	X (forward)	Y (right)	Z (down)
CHII (Topo and Shallow Channel)	Reference to GNSS Antenna L1 Phase Center	0.597 m	-0.066	-1.226
	Reference to IMU	-0.003 m	-0.006 m	-0.296 m
	Reference to IMU Rotation	0°	0°	90°
Deep Channel	IMU to GNSS Antenna L1 Phase Center	1.269	-0.140	-0.819
	Reference to IMU Rotation	0°	90°	-90°

2.2. Lidar Calibration

Field calibration of the HE4X system is carried out to eliminate systematic errors by calculating corrections for boresight errors, scanner angle errors, remaining IMU angle errors and any necessary internal timing errors. In order to verify or compute the field calibration, the following lines are flown (Figure 3):

a. 2 x Line A over mixed terrain with flat or gentle slopes and features such as peaked roof buildings (1 x each direction)
b. 1 x Line B offset +50% from Line A in one direction
c. 1 x Line C offset -50% from Line A in the same direction as Line B
d. 2 x Line D orthogonal to previous lines (1 x each direction)

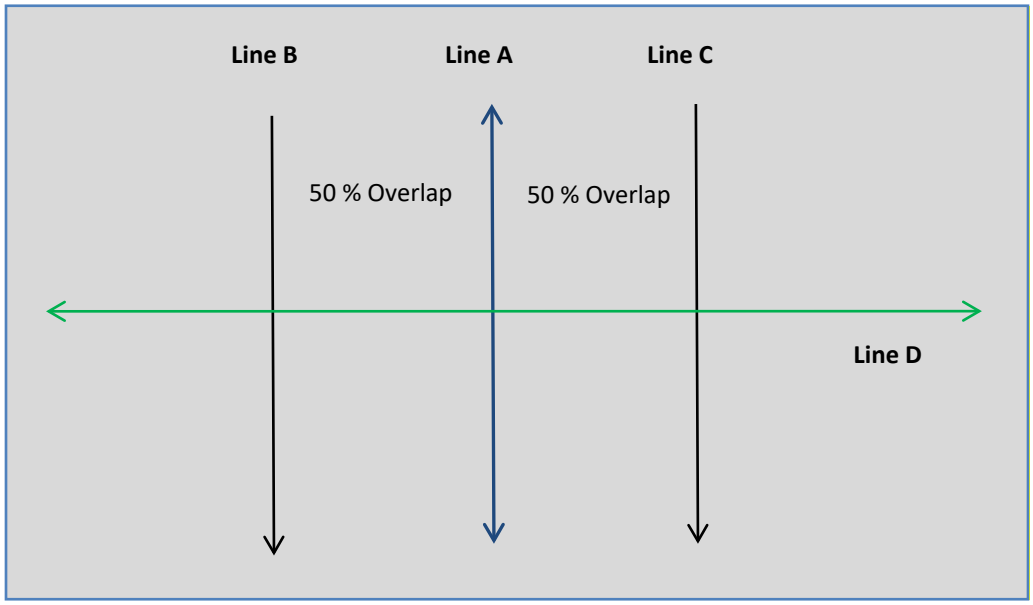

Figure 3: Schematic of HE3 Calibration Lines

A set of calibration lines were acquired at 500m, and 400m altitude for all calibration flights. The February 23, 2020 flight also included a set acquired at 800m altitude while the July 14, 2020 flight included a set at 600m altitude. All sets of lines are used to calibrate and verify the topographic lidar, while the 500m and 400m lines are used for the bathymetric lidar.

Calibration values are calculated using the automatic calibration routine within the Leica Lidar Survey Studio (LSS) software. This utility first identifies patches or areas of gentle slope within the overlap region of all the lines to use for calibration. Patch selection prevents areas of vegetation, side of cars or buildings, from being used in the calibration process. Next, the utility compares the front side and back side of the elliptical scan within the same line, as well as comparing all lines to each other, to identify suitable calibration parameters such that data within the patches match. The procedure is iterative and continues until the best possible solution is computed.

Calibration for each channel (topo, shallow, and deep) is done independently. Topo channel calibration was computed using 500m altitude lines. Any other altitude data was then used for verification. Calibration of the shallow and deep channel were computed using 500m altitude. Any lower altitude data were used for verification.

At each step of the calibration process, quality assurance is conducted to ensure values being calculated are valid. This is done using the Leica LSS Quality Control Utility. Two types of checks are done; firstly, the front scan is compared to the back scan for every line. Secondly, a single line is chosen as a baseline and is compared to every other line. We would expect the average errors from both checks to be small; less than 2cm. In addition, the data is visually reviewed. In particular, features are studied to ensure lines from different directions show structures in the same position, in other words, verifying horizontal accuracy is maintained. These tests all provide assurance of relative accuracy.

Ground truth is not used within the automatic calibration routine; however, ground truth can be used to verify absolute accuracy.

For this project, calibration lines were acquired over an urban area on the island of Saipan for all three calibration flights. Results from each full calibration are provided in Tables Table 3Table 4Table 5. Results are good and indicate that calibration was successful. Values computed were used for the entire project.

Table 3: August 25, 2019 Calibration QA Results

Test		Topo 500m	Topo 400m	Shallow 500m	Shallow 400m	Deep 500m	Deep 400m
Front to Back Scan Comparison	Average Error (m)	-0.0023	-0.0067	-0.0030	-0.0131	-0.0051	0.0084
	Std. Dev. of Error	0.0002	0.0004	0.0012	0.0017	0.0011	0.0023
Line to Line Comparison	Average Error (m)	-0.0188	-0.0106	-0.0179	-0.0185	-0.0138	-0.0138
	Std. Dev. of Error	0.0021	0.0020	0.0014	0.0019	0.0050	0.0050

Table 4: February 23, 2020 Calibration QA Results

Test		Topo 800m	Topo 500m	Topo 400m	Shallow 500m	Shallow 400m	Deep 500m	Deep 400m
Front to Back Scan Comparison	Average Error (m)	0.0066	0.0004	0.0028	0.0039	0.0053	0.0009	0.0168
	Std. Dev. of Error	0.0009	0.0007	0.0008	0.0026	0.0031	0.0018	0.0026
Line to Line Comparison	Average Error (m)	0.0355	0.0083	0.0030	0.0048	0.0016	-0.0025	0.0042
	Std. Dev. of Error	0.0053	0.0050	0.0021	0.0019	0.0084	0.0064	0.0071

Table 5: July 14, 2020 Calibration QA Results

Test		Topo 600m	Topo 500m	Topo 400m	Shallow 500m	Shallow 400m	Deep 500m	Deep 400m
Front to Back Scan Comparison	Average Error (m)	-0.0011	-0.0003	-0.0032	-0.0010	-0.0054	0.0049	0.0099
	Std. Dev. of Error	0.0004	0.0005	0.0004	0.0029	0.0024	0.0052	0.0023
Line to Line Comparison	Average Error (m)	-0.0016	-0.0122	-0.0053	-0.0120	-0.0074	-0.0109	-0.0043
	Std. Dev. of Error	0.0025	-0.0015	0.0016	0.0029	0.0030	0.0036	0.0027

Woolpert acquired a set of ground truth points with Real Time Kinematic (RTK) GNSS within the calibration area on August 23, 2019. Ground truth is not used within the automatic calibration routine; however, a comparison to the lidar data was used to verify absolute accuracy. Results presented in Table 6, Table 7, and Table 8 show data is well within required accuracy specifications.

Table 6: August 25, 2019 Calibration Ground Truth Comparisons

	Topo		Shallow		Deep	
	500m	400m	500m	400m	500m	400m
Average dz (m)	-0.0052	0.0064	-0.0196	0.0158	-0.0434	-0.0052
Root Mean Square (m)	0.0161	0.0178	0.0238	0.0453	0.0400	0.0448

Table 7: February 23, 2020 Calibration Ground Truth Comparisons

	Topo			Shallow		Deep	
	800m	500m	400m	500m	400m	500m	400m
Average dz (m)	0.0072	0.0018	-0.0246	0.0035	0.0042	0.0195	-0.0188
Root Mean Square (m)	0.0270	0.0360	0.0320	0.0301	0.0191	0.0383	0.0363

Table 8: July 14, 2020 Calibration Ground Truth Comparisons

	Topo			Shallow		Deep	
	600m	500m	400m	500m	400m	500m	400m
Average dz (m)	-0.0012	0.0100	0.0232	0.0066	0.0060	0.0256	0.0406
Root Mean Square (m)	0.0115	0.0096	0.0237	0.0181	0.0231	0.0245	0.0382

2.3. AERIAL SURVEY OPERATIONS

For ease of operations and data management, the survey area was split into twelve survey blocks (BL). Actual flight lines flown, including start and end data along with unique line ID, are provided in the flight line database included with the project deliverables. A summary of the daily operations is shown in Table 9. Detailed Flight Logs for each day are provided in Appendix A.

Table 9: Summary of Daily Operations

Flight (UTC Dates)	Engine Time	Air Time	Flown		Reflown		Comments
			km	%	km	%	
2019-07-04A							Pilot Transit to Saipan
2019-07-05A	5:27:00	5:00:00	487.3	12.9%	96.4	2.6%	BL03 (FdM), BL05 (Saipan)
2019-07-06A	1:05:00	0:45:00			16.1	0.4%	BL03 (FdM), BL05 (Saipan)
2019-07-06B	4:55:00	4:51:00	317.6	8.4%	13.4	0.4%	BL01, BL02 (Pagan)
2019-07-07A	5:37:00	5:14:00	234.2	6.2%	32.7	0.9%	BL01, BL02 (Pagan), BL04 (Saipan)
2019-07-08A	5:22:00	5:06:00	568.1	15.1%			BL04, BL05, BL06 (Saipan)
2019-07-09A							Weather
2019-07-10A							Weather
2019-07-11A	4:54:00	4:25:00	397.8	10.6%	62.1	1.6%	BL04, BL05, BL06 (Saipan), BL07 (Tinian)
2019-07-12A	0:47:00	0:35:00	59.8	1.6%	18.0	0.5%	BL06 (Saipan)
2019-07-12B	3:57:00	3:54:00	364.0	9.7%	46.7	1.2%	BL06 (Saipan), BL07, BL08 (Tinian), BL09, BL10 (Aguijan)
2019-07-13A	2:44:00	2:25:00	238.9	6.3%	44.7	1.2%	BL06 (Saipan)
2019-07-13B	2:07:00	2:04:00	102.7	2.7%	71.9	1.9%	BL08 (Tinian), BL11 (Rota)
2019-07-14A	2:38:00	2:04:00	106.3	2.8%	6.2	0.2%	BL11 (Rota)
2019-07-16A	1:00:00	0:39:00			85.3	2.3%	BL04, BL05 (Saipan)
2019-07-16B	1:21:00	0:59:00			96.7	2.6%	BL05 (Saipan)
2019-07-17A							Aircraft Maintenance, Weather
2019-07-18A	2:26:00	2:04:00			270.8	7.2%	BL05 (Saipan), BL07 (Tinian)
2019-07-20A	1:27:00	0:51:00			58.4	1.6%	BL04 (Saipan)
2019-07-20B	2:43:00	2:27:00			126.0	3.3%	BL05 (Saipan)
2019-07-21A	3:29:00	3:04:00			317.0	8.4%	BL04 (Saipan)
2019-07-22A	3:06:00	2:45:00	123.5	3.3%	23.5	0.6%	BL11 (Rota)

2019-07-22B	2:27:00	2:06:00			47.8	1.3%	BL06 (Saipan)
2019-07-22C	2:27:00	2:06:00	87.8	2.3%	55.8	1.5%	BL06 (Saipan)
2019-07-23A	1:55:00	1:32:00	11.3	0.3%	104.0	2.8%	BL04 (Saipan)
2019-07-23B							Weather / Rain and Low Clouds
2019-07-24A	5:59:00	5:24:00	371.6	9.9%	54.2	1.4%	BL04-BL06 (Saipan), BL11, BL12 (Rota)
2019-07-25A	3:33:00	2:39:00	134.3	3.6%	17.5	0.5%	BL08, (Tinian), BL12 (Rota)
2019-07-26A	2:44:00	2:10:00			119.6	3.2%	BL03 (FdM)
2019-07-27A	3:09:00	2:50:00	128.7	3.4%	38.1	1.0%	BL06 (Saipan), BL08 (Tinian), BL12 (Rota)
2019-07-28A	5:57:00	5:35:00			331.5	8.8%	BL01, BL02 (Saipan), BL08 (Tinian)
2019-07-29A							Weather / Rain and Low Clouds
2019-07-30A	5:23:00	5:07:00			262.4	7.0%	BL01, BL02 (Pagan)
2019-07-31A	4:00:00	3:21:00			187.6	5.0%	BL04, BL06, (Saipan), BL07, BL08 (Tinian), BL09, BL10 (Aguijan), BL11, BL12 (Rota)
2019-08-01A							Weather
2019-08-02A	3:46:00	3:23:00			82.3	2.2%	BL01, BL02 (Pagan)
2019-08-03A	4:20:00	3:57:00			98.6	2.6%	BL02 (Pagan)
2019-08-04A							Weather / Rain and High Winds
2019-08-05A							Weather / Rain and High Winds
2019-08-06A							Weather / Rain and High Winds
2019-08-07A	3:14:00	2:54:00			118.0	3.1%	BL04, BL05, BL06 (Saipan), BL12 (Rota)
2019-08-08A	2:47:00	2:28:00			111.5	3.0%	BL04, BL05, BL06 (Saipan)
2019-08-09A	1:11:00	0:51:00			45.8	1.2%	BL06 (Saipan)
2019-08-10A							Weather / Low Clouds
2019-08-11A							Weather / Low Clouds
2019-08-12A							Weather / Low Clouds
2019-08-13A	3:02:00	2:44:00			12.3	0.3%	BL02 (Pagan), BL12 (Rota)
2019-08-14A	1:04:00	0:43:00			22.3	0.6%	BL05 (Saipan)
2019-08-14B	0:42:00	0:23:00			15.4	0.4%	BL05 (Saipan)
2019-08-15A							Weather / Low Clouds
2019-08-16A							Weather / Low Clouds
2019-08-17A							Weather / Low Clouds
2019-08-18A							Weather / Low Clouds
2019-08-20A	3:30:00	3:04:00			19.0	0.5%	BL02 (Pagan)
2019-08-21A	1:25:00	0:53:00			36.7	1.0%	BL04, BL05 (Saipan)
2019-08-25A	2:15:00	1:46:00			178.2	4.7%	BL04, BL05 (Saipan)
2020-02-12A	1:17:00	0:48:00					

2020-02-15B	5:04:00	4:36:00			86.8	2.3%	BL02 (Pagan)
2020-02-16A	4:04:00	3:39:00			32.6	0.9%	BL02 (Pagan)
2020-02-19A	2:03:00	1:38:00	5.7	0.2%	17.6	0.5%	BL12 (Rota)
2020-02-19B	5:23:00	4:54:00	55.9	1.5%	4.0	0.1%	BL02 (Pagan), BL12 (Rota)
2020-02-20A	1:10:00	0:38:00					BL12 (Rota)
2020-02-21A	0:57:00	0:38:00					
2020-02-21B	0:55:00	0:36:00					
2020-02-22A	1:07:00	0:39:00					
2020-02-23A	4:16:00	3:51:00			15.6	0.4%	BL02 (Pagan)
2020-02-23A	4:16:00	3:51:00	2.0	0.1%	15.6	0.4%	BL02 (Pagan)
2020-02-23B	1:18:00	0:55:00	6.6	0.2%	6.2	0.2%	BL12 (Rota)
2020-02-23C	2:23:00	2:02:00			217.7	5.8%	Cal
2020-02-26A	3:48:00	3:28:00	2.0	0.1%	4.0	0.1%	BL02 (Pagan)
2020-06-19A	2:02:00	1:44:00			66.0	1.8%	Cal
2020-07-02A	4:11:00	3:54:00			26.7	0.7%	BL01, BL02 (Pagan)
2020-07-04A	1:25:00	1:04:00					BL12 (Rota)
2020-07-05A	0:46:00	0:21:00			10.5	0.3%	Cal
2020-07-05B	1:02:00	0:45:00					BL12 (Rota)
2020-07-11A	2:08:00	1:24:00			238.8	6.3%	Cal
2020-07-11B	1:17:00	0:57:00	21.7	0.6%	238.8	6.3%	BL12 (Rota)
2020-07-14A	2:07:00	1:15:00			231.3	6.1%	Cal
TOTAL	**172:54:00**	**148:45:00**	**3828**	**101.7%**	**4556**	**121.0%**	

2.3.1. THE HAWKEYE 4X SENSOR

All lidar data were acquired using a HE4X sensor (Figure 4). The HE4X is a latest generation topographic and bathymetric lidar sensor. The system provides denser data than previous traditional bathymetric lidar systems. It is unique in its ability to acquire bathymetric lidar, topographic lidar and 4-band digital camera imagery simultaneously.

The HE4X provided up to 500 kHz topographic data and an effective 140 kHz shallow bathymetric data and a 40 kHz deep channel. While not a required deliverable for this survey, 4-band 80 MP digital camera imagery was also collected simultaneously with the sensor's RCD-30 camera and utilized during data editing in some cases.

The bathymetric and topographic lasers are independent and do not share an optical chain or receivers, so they are optimized for their specific function. As with any bathymetric lidar, maximum depth penetration is a function of water clarity and seabed reflectivity. The HE4X is designed to penetrate to 3 times the secchi depth. This is also represented as Dmax = 4/K, where K is the diffuse attenuation coefficient, and assuming K is between 0.1 and 0.3, a normal sea state and 15% seabed reflectance.

Both the topographic and bathymetric sub-systems use a palmer scanner to produce an elliptical scan pattern of laser points with a degree of incidence ranging from +/-14° (front and back) to +/-20° (sides), providing a 40° field of view. This has the benefit of providing multiple look angles on a single pass and helps to eliminate shadowing effects. This can be of particular use in urban areas, where all sides of a building are illuminated, or for bathymetric features such as the sides of narrow water channels, or features on the seafloor such as smaller objects and wrecks. It also assists with penetration in the surf zone where the back scan passes the same ground location a couple of seconds after the front scan, allowing the areas of whitewater to shift.

Figure 4: Hawkeye 4X Bathymetric Lidar Sensor Installation

For this project, the flight parameters shown in Table 10 were used. Flight lines were planned to provide 100% coverage using a 15% sidelap for the topo and 20% sidelap for the bathymetry.

During acquisition, flight lines are shown on a pilot's display, and the aircraft is controlled by the pilots at all times. The HE4X system includes a NovAtel SPAN GNSS system with an LCI-100C IMU for aircraft position and orientation. The IMU is in the main Chiroptera sensor head, which includes the topo channel, shallow channel and RCD30 camera. Information from this IMU is also used in real-time by the PAV100 gyro-stabilized mount to compensate for deviations in pitch and roll. Aircraft bank angles were restricted to 20º to avoid any potential GNSS dropouts. No flights were planned if the PDOP was expected to go above 3.0.

Data were monitored for quality during acquisition using the Operators Console running on the AHAB collection computer. The operator monitored system status of the scanners and receivers, waveforms, camera images, data coverage, flight lines and the health of the navigation system.

All data were recorded to a removable solid-state hard disk. At the end of the flight the hard disk was removed and taken to the field office where data was copied on to backup disks for transmittal back to the main processing office. Data is reviewed daily in the field for quality and coverage to ensure that voids due to gaps between data swaths, instrument malfunction, insufficient return amplitude, or cloud cover/ground fog are re-captured. However, unavoidable voids due to exceptionally low reflectivity (composition roofing; wet asphalt paving; and shadowing by forest canopy) may occur.

Table 10: Survey Flight Parameters

System	
Aerial System	Leica Hawkeye 4X (topo-bathy)
Nominal Survey Altitude	480/600m (1575/1969 feet)
Nominal Survey Speed	130 knots
System Planned Sidelap	15% Topo / 20% Bathy
Lidar	

Scan Angle	≤ 40° (+/-20° from Nadir)
Nominal Swath Width	350m (1148 ft) at 480m altitude 435m (1427 ft) at 600m altitude
PRF (Topo)	450/500 kHz
Effective PRF (Shallow)	140 kHz
Effective PRD (Deep)	40 kHz
Pulse Density (Topo)	≥ 8 pulses/m^2 (≤ 0.35 m NPS)
Pulse Density (Bathy)	≥ 2 pulses/m^2 (≤ 0.71 m NPS)
Returns Collected Per Laser Pulse (Topo)	Up to 4
Returns Collected Per Laser Pulse (Bathy)	Up to 4
Intensity Range	0 – 65535 (16-bit)

2.3.2. POSITIONING

Position and orientation data were acquired in the aircraft using a NovAtel SPAN with LCI-100C IMU. All data were post-processed using NovAtel Inertial Explorer software to provide a tightly coupled position and orientation solution.

A single base station was used to control trajectory processing providing final trajectories for Saipan and Tinian on NAD83 (MA11), Epoch 2010, located in the Saipan airport. This base station was replaced for each of the three separate collects of the project (Table 11). SPN1, SPN2 and SPN3 were occupied with a Trimble GNSS receiver by Woolpert. Due to the distance of Rota, Aguijan, Farallon de Medinilla, and Pagan from the single base station on Saipan and their remoteness a precise point positioning (PPP) solution was used for them on ITRF2014.

To establish a reliable coordinate for SPN1 data were uploaded to the National Geodetic Service (NGS) Online Positioning User Service (OPUS), and for SPN2 and SPN3 Trimble CenterPoint RTX Post-Processing service was used. The average OPUS or RTX coordinate from multiple days of observations was used to process the final trajectories.

Logs for the trajectory processing are provided in Appendix B.

Table 11: GNSS Base Stations Used for Trajectory Processing, NAD83 (MA11) Epoch 2010.0

GNSS Base Station	Latitude	Longitude	Height (m)	Source
SPN1	15° 07' 12.38779"N	145° 43' 15.98811"N	116.756	OPUS
SPN2	15° 07' 12.35969"N	145° 43' 15.95277"N	116.789	RTX
SPN3	15° 07' 12.29815"N	145° 43' 16.16988"N	116.806	RTX

2.3.3. PPP SHIFTS

In order to account for any potential trajectory shifts between each survey day for flights processed with PPP trajectories over Pagan, Farallon de Medinilla, Aguijan, and Rota, QC data were acquired over single base survey data on Saipan island across the acquisition period.

The single base survey data on Saipan island was masked to areas of only return with a slope less than 10 degrees and compared to each lidar PPP QC line processed with PPP trajectory. A shift per line was computed and averaged across all lines for each island. During lidar processing any line to line vertical mismatches are removed, therefore, an average PPP shift per island was computed and applied to remove any remaining errors in the ellipsoid height due to the use of PPP processing of the trajectories. Results for each island are presented in Table 12.

Table 12: Corrections for PPP Shift

Survey Area	PPP Shift Applied to Lidar Data (m)
Pagan	0.105

FdM	0.087
Aguijan	0.087
Rota	0.081

2.4. Ground Survey Operations

Ground control surveys were conducted to support the airborne acquisition. Ground control surveys were conducted to assist with final flight line calibration.

2.4.1. Primary Control Points

Woolpert used local GNSS base stations or precise point positioning (PPP) to conduct final trajectory processing as described in Section 2.3.2.

2.4.2. Lidar Ground Survey Points (GSPs)

Ground survey points (GSPs) were collected using traditional GNSS-based real time kinematic (RTK) survey techniques on Saipan, Tinian, and Rota. These points were used to remove any vertical bias in the lidar data.

The GSPs were all collected on bare earth surfaces on a level slope. Areas on elevated road structures (bridges, large culverts, etc.), were avoided.

2.4.3. Lidar Ground Check Points (GCPs)

Ground check points (GCPs) were not collected by Woolpert. The National Oceanic and Atmospheric Administration (NOAA) will be analyzing check points. These points are distinct from GSPs and will not be used to correct the lidar data in any way.

3. DATA PROCESSING

An overview of Woolpert's established HE4X processing workflow is presented in Figure 5. Initial data coverage analysis and quality checks to ensure there were no potential system issues were carried out in the field prior to demobilization of the sensor. Final processing was conducted in Woolpert's offices.

In general data were initially processed in Leica's Lidar Survey Studio (LSS) using final processed trajectory information. LAS files from LSS were then imported to a Terrascan project where spatial algorithms were used to remove noise and classify bare earth/ground. Manual review was conducted in both Terrascan and LP360 prior to product creation.

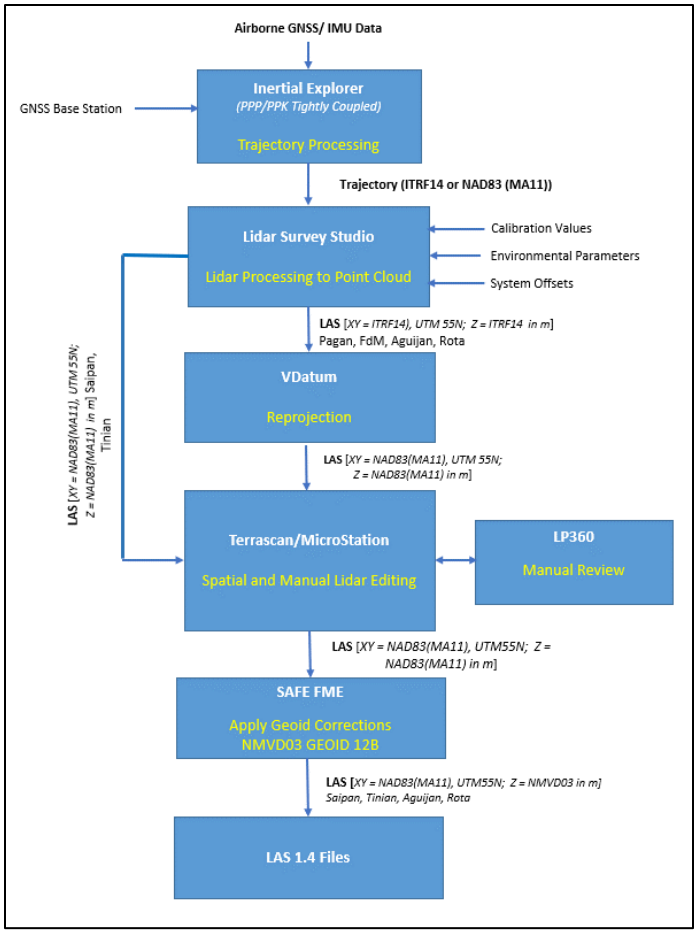

Figure 5: Overview of Processing Workflow

3.1. POSITION

Final trajectory data were post processed in NovAtel Inertial Explorer. Lever arms, shown in the NovAtel reference frame, are presented in Table 13. Inertial Explorer accounts for the fixed offset between the reference point and IMU and uses a multi-pass algorithm to compute a tightly coupled solution. GNSS base stations and precise point positioning (PPP) were used for processing, as described in Section 2.3.2. Trajectory processing logs are provided in Appendix B. Average Forward and Reverse Separation RMS for the project was 0.013m in Easting, 0.014m in Northing, and 0.043m in Height for single base solutions.

Table 13: Inertial Explorer Offsets

Sensor Head	Lever Arm	X (right)	Y (forward)	Z (up)
Chiroptera (Topo, Shallow)	Reference to GNSS Antenna L1 Phase Center	-0.061 m	0.600 m	0.930 m
	Reference to IMU Rotation	0 °	180 °	0 °
Deep Channel	Reference to GNSS Antenna L1 Phase Center	-0.140	1.269	0.819
	Reference to IMU Rotation	-90 °	0 °	180 °

3.2. LIDAR

3.2.1. RAW DATA PROCESSING

Lidar processing was conducted using the Leica Lidar Survey Studio (LSS) software. Calibration information, along with processed trajectory information were combined with the raw laser data to create an accurately georeferenced lidar point cloud for the entire survey in LAS v1.4 format. All points from the topographic and bathymetric laser include 16-bit intensity values.

During this LSS processing stage, an automatic land/water discrimination is made for the bathymetric waveforms. This allows the bathymetric (green) pulses over water to be automatically refracted for the pulse hitting the water surface and travelling through the water column, producing the correct depth. Another advantage of the automatic land/water discrimination is that it permits calculation of an accurate water surface over smaller areas, allowing simple bathymetric processing of smaller, narrower streams and drainage channels. Sloping water surfaces are also handled correctly.

Prior to processing, the hydrographer can adjust waveform sensitivity settings dependent on the environment encountered and enter a value for the refraction index to be used for bathymetry. The index of refraction is an indication of the water type. Values used for sensitivity settings and the index of refraction are included in the LSS processing settings files. A value of 1.34206 was used for the index of refraction, indicating saltwater.

In the field, default waveform sensitivity settings were used for processing. In order to determine the optimal waveform sensitivity settings for final processing, sample areas were selected and processed with multiple different settings, to iteratively converge on the best possible settings. This is done by reviewing the processed point cloud and waveforms within sample areas. A sample waveform is provided in Figure 6, while a sample LSS editing screen is provided in Figure 7. Settings affect which waveform peaks are classified as valid seabed, and which peaks are classified as noise. Optimal settings strike a balance between the amount of valid data that is classified as seabed bottom, and the amount of noise that is incorrectly classified due to peaks in the waveforms. Ideally all valid data is selected, while only a small amount of noise remains to be edited out. Once optimal threshold settings were chosen, these were used for the entire project.

It is important to note that all digitized waveform peaks are available to be reviewed by the hydrographer; both valid seabed bottom and peaks classed as noise. This allows the hydrographer to review data during TerraScan and LP360 editing for valid data such as objects that may have been misclassified as noise.

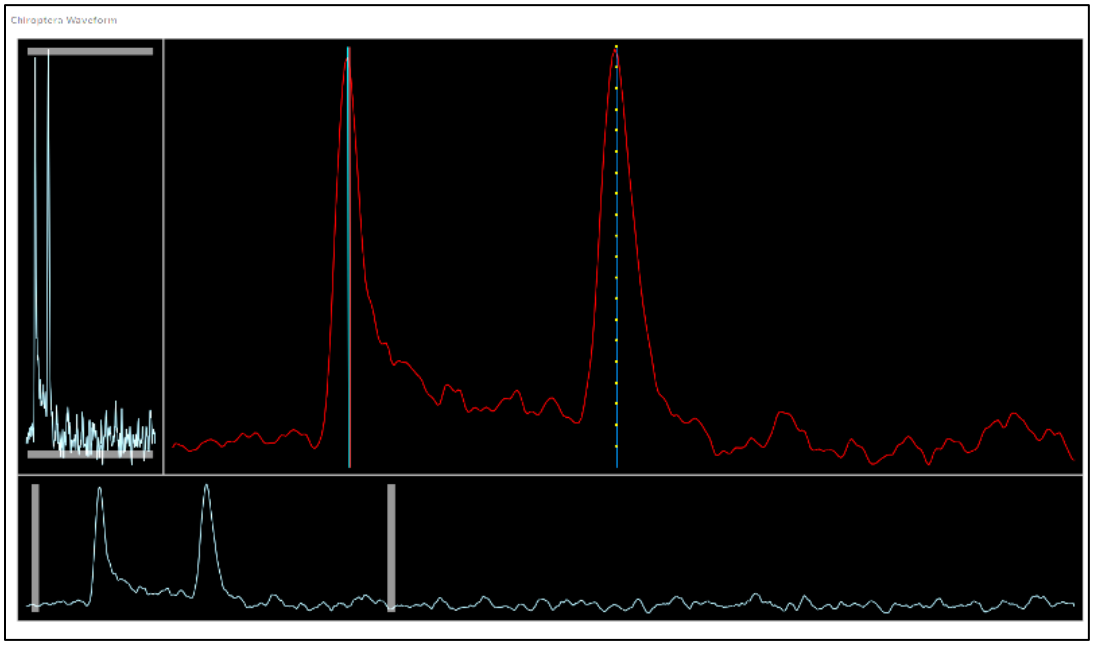

Figure 6: Sample Waveform in Shallow Water

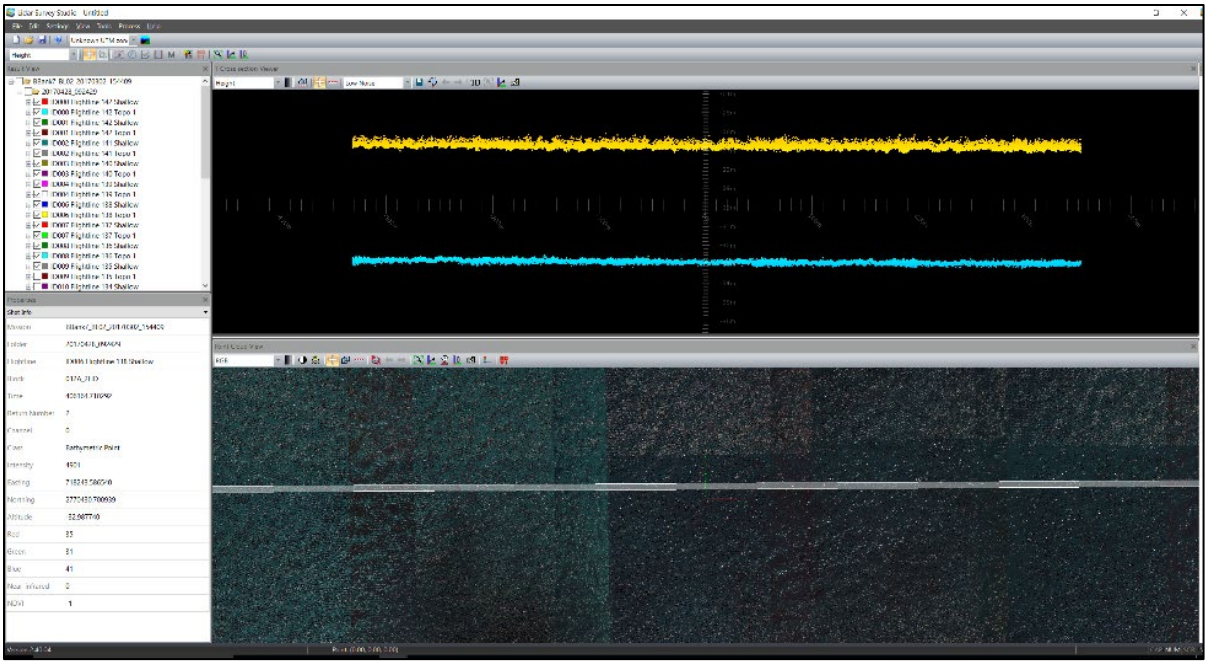

Figure 7: Sample LSS Processing Screen

LSS processing produced LAS files in 1.4 format.

Additional QC steps were performed prior to import to TerraScan. Firstly, the derived water surface was reviewed to ensure a water surface was correctly calculated for all bathymetry channels. No significant issues were apparent.

Spot checks were also made on the data to ensure the front and back of the scans remained in alignment and no calibration or system issues were apparent prior to further data editing in TerraScan.

LSS Processing Logs are provided in Appendix B.

LSS stores data in multiple LAS files for a single flight line. Each file corresponds to a single .dat file from the raw airborne data. Woolpert merged these multiple files into a single file per flight line and moved data into a standard class definition in preparation for data editing using Woolpert's proprietary scripts within SAFE's FME software.

Data produced by LSS for flights over Saipan and Tinian were processed on the NAD83 (MA11) Epoch 2010 datum in UTM 55N Zone with units in meters, and elevations on the ellipsoid also in meters. Data produced for Pagan, Farallon de Medinilla, Aguijan and Rota were processed on the ITRF2014 datum in UTM 55N Zone with units in meters, with elevations on the ellipsoid also in meters.

3.2.2. LIDAR DATA EDITING

After data were processed in LSS and the data integrity reviewed, Pagan, Farallon de Medinilla, Aguijan, and Rota were transformed from the ITRF2014 ellipsoid to the NAD83 (MA11) Epoch 2010 ellipsoid using VDatum. With the entire project now on the correct ellipsoid, data were organized into tiles within a TerraScan project. The tile layout is the same as that provided with the project deliverables.

Data classification and spatial algorithms were applied in Terrasolid's TerraScan software. Customized spatial algorithms, such as isolated points and low point filters, were run to remove gross fliers in the topographic and bathymetric data. A grounding algorithm was also run on the topographic data to distinguish between points representing the bare earth, and other valid topo lidar points representing features such as vegetation, buildings, and so forth. Algorithms were run on the entire dataset.

Data were reviewed manually to reclassify any valid bathy points incorrectly identified by the automated routines in LSS as invalid, and vice versa. In addition, any topo points over the water were reclassified to correct the ground representation. Manual editing was conducted both in TerraScan and LP360. Steps for manual editing included:

- Re-class any topo unclassified laser data and bathy seabed data from the water surface to a water surface class
- Review bathymetry in cross section.
    - Re-class suitable data to Seabed (Class 40).
    - Re-class any noise in the bathy ground class to bathy noise (Class 45).
- Review topo ground points in areas of gaps or spikes.
    - Add points to ground (Class 2) from the topo laser if points are available to fill gaps in the ground model.
    - Re-class any noise in the ground class to Topo Unclassified (Class 1) if valid vegetation or other feature, or Noise if the point is not valid (Low Noise (Class 7) or High Noise (Class 18)).
- Review topo ground points for bridges and re-class to Bridge Deck (Class 17).
- Review bathymetry using imagery and nautical charts and re-class obvious man-made objects to Submerged Object (Class 43).

Once editing was completed in TerraScan the islands of Saipan, Tinian, Aguijan, and Rota were vertically transformed to the NMVD03 datum using GEOID12B. Pagan and Rota were not transformed as they were outside the GEOID12B extents and retained NAD83(MA11) ellipsoid heights.

Digital Elevation Models (DEMs) were then created using TerraModel at 1m resolution using Topo Ground, Seabed, and Submerged Object classes. (Class 2, 40, and 43).

The topo data was then reviewed for inland water bodies larger than 2 acres and for streams wider than 100 feet. These water bodies were hydro-flattened. Breaklines around inland water meeting the hydro-flattening requirements were digitized and a second set of DEMs were created using TerraModel at 1m resolution using Topo Ground (Class 2) and digitized breaklines for all islands. Only Pagan and Saipan contained water bodies requiring hydro-flattening.

3.3. REFLECTANCE

Although the bathymetry data includes intensity values, these are raw values. For intensity (reflectance) to correctly represent the reflectance of the seabed, the intensities must be normalized for any losses in signal as the light travels through the water column, so that the intensity value better reflects the intensity of the seabed itself.

One of the fundamental issues that exists with reflectance imagery is the variance in return due to water clarity differences occurring spatially along line, and temporally from day to day. This is challenging for any bathymetric lidar sensor.

If water clarity is relatively consistent along a line, then it is possible to achieve an overall homogenous reflectance image for an area. To a certain extent, variation in reflectivity intensity can be minimized by limiting the size of flight blocks and trying to ensure similar environmental parameters exist within a single flight block. In other words, where changes in water clarity or environment may be expected, flight blocks should be split to allow different normalization parameters to be used per block for the reflectance processing. Where this is not possible, and water clarity varies significantly along a line, variation in reflective intensity will be seen in the output imagery. While this imagery can still be analyzed and used for manual seabed classification, it prohibits the use of unsupervised, or semi-automated classification.

For this survey, cloud shadows (ambient light) had an effect on the resulting reflectance images.

Woolpert used proprietary in-house scripts developed in MATLAB to compute project specific correction parameters and normalize the raw intensity data for depth. This provides intensities that more closely represent the reflectance of the actual seabed. Corrected values were used to create 1m reflectance images per flightline using Applied Imagery's QT Modeler software. Individual flightline reflectance images were then used in Trimble's OrthoVista software to create a final reflectance image for the entire area.

OrthoVista was used to improve radiometric balancing between lines and the seamline editor was used to improve the joins between lines to remove as much line to line edge matching and cloud artifact issues as possible.

4. QUALITY CONTROL

Quality control is carried out through every phase of the project. Several checks were used to ensure data integrity and quality was maintained.

4.1. CALIBRATION

This is fundamental to good data accuracy. Calibration is discussed in detail in Section 2.2.

4.2. ONLINE CHECKS

The airborne operator monitored system status of the scanners and receivers, waveforms, camera images, data coverage, flight lines and health of the navigation system during data acquisition. Flight logs are maintained during data acquisition. Logs not only track lines acquired, but also any relevant information on weather or water clarity, instances when sensor issues occur and so on. These logs are a valuable resource during processing. They are provided in Appendix A.

4.3. POSITIONING

During acquisition, aircraft bank angles were restricted to 20º to avoid any potential GNSS dropouts. No flights were planned if the PDOP was expected to go above 3.0. Separation plots and additional statistics were reviewed for each flight trajectory processed.

4.4. TOPO COMPARISON TO ADJACENT LINES

Throughout data editing adjacent survey lines of data are compared to ensure there are no data busts, or system artifacts. During processing Terrasolid's TMatch software is run to examine the Delta Z differences between overlapping lines. If differences are greater than 0.02m, then a simple Z correction is applied per flight line to remove any vertical differences between flight lines. TMatch can then be run again once all corrections are applied to ensure adjacent lines agree within specification. This provides a measure of inter-swath accuracy. Fluctuation corrections were also run due to strong vertical differences throughout the flightline.

Overlap consistency was also measured by generating a grid at 2m using single returns in areas with less than 10 degrees of slope. The average relative accuracy of the lidar data for the project measured at 0.049 meters RMSDz with over 6 million samples measured. All differences per island are within specification (RMSDz <0.08m). Results for each island are shown in Table 14.

Table 14: Overlap Consistency

Survey Area	Count	Mean (m)	St Dev	RMSDz
Pagan	556930	0.0003	0.0692	0.069
FdM	7857	-0.0007	0.0677	0.068
Saipan	3212122	-0.0005	0.0328	0.033
Tinian	1119535	0.0015	0.0433	0.043
Aguijan	112140	-0.0004	0.0493	0.049
Rota	1434410	0.0002	0.0317	0.032

4.5. BATHY CROSSLINE ANALYSIS

Crosslines were run in a direction perpendicular to main scheme lines across the entire survey area, provided a good representation for analysis of consistency. All crosslines were used for crossline comparisons.

Crossline analysis was performed using the Fledermaus CrossCheck tool. Crossline point data were compared to a 1m gridded surface of the main scheme survey lines and statistics generated. Slopes greater than 10 degrees were excluded from the analysis. For each line, a histogram of the point comparison was reviewed in CrossCheck to ensure there was a normal distribution of data. A summary of the CrossCheck results is provided below. The result of the analysis meets the required National Coastal Mapping Strategy QL2b requirements.

Table 15: Cross Line Point to Surface Results

No. of Points Compared	27,471,390
Mean Difference (MD) in m	0.002
Standard Deviation (St. Dev)	0.121
Mean + 2* Std. Dev	0.244

In addition, 1m surfaces were created for the crosslines, and surface differences generated between the crossline and main scheme surfaces. Statistics for the difference surfaces were generated. Results matched those from the CrossCheck analysis, as shown below.

Table 16: Crossline Surface Difference Results

Mean Difference (m)	0.001
St. Dev	0.136

4.6. Absolute Vertical Accuracy Checks

Absolute vertical accuracy checks will be carried out by NOAA. No check points will be used to adjust the lidar data.

5. DELIVERABLES

All data are provided in the project datum and coordinate system provided in Table 17.

Table 17: Project Datum and Projection

Horizontal Datum	NAD83 (MA11) Epoch 2010.0
Vertical Datum	NMVD03 (Geoid 12B)
Projection	UTM 55N
Units (Horizontal and Vertical)	Meters

All deliverables listed in Table 18 are provided on a USB3 hard drive. The deliverables meet the required accuracy specifications.

All products are accompanied by FGDC compliant metadata, verified using the USGS Metadata Parser.

Table 18: Lidar Product Deliverables

Delivery Lot	Folder	Subfolder	Format	Cell Size	Contents
211535	**metadata**	reports	GeoTIFF	1m	Final bare earth raster files by island
		shapefiles	SHP	--	Supplemental shapefiles
	bare_earth	be_rasters	GeoTIFF	1m	Final bare earth raster files by island

	other	intensity	GeoTIFF	1m	Final intensity raster files by island
	point_cloud	tilecls	LAS 1.4 PDRF 6	--	Classified point cloud LAS files by island
211610	**metadata**	reports	GeoTIFF	1m	Final bare earth raster files by island
		shapefiles	SHP	--	Supplemental shapefiles
	bare_earth	be_rasters	GeoTIFF	1m	Final bare earth raster files by island
		breaklines	SHP		Breaklines use to create the bare earth rasters
	other	intensity	GeoTIFF	1m	Final intensity raster files by island
	point_cloud	tilecls	LAS 1.4 PDRF 6	--	Classified point cloud LAS files by island
other			SHP	--	Points used to control the survey.

In addition to the deliverables listed in Table 18 the project survey report is located in the root folder of the USB3 drive in PDF format.

5.1. Classified Point Cloud (LAS Files)

The classified point cloud LAS 1.4 files are delivered using standard ASPRS Classification Levels, with the LAS Topo-Bathy Domain Profile (July 17, 2013) classes. Final LAS classes included are provided in Table 19.

All LAS files include intensity values Therefore, all data are in Point Record Format 6.

Table 19: Delivered LAS Classes

Class Number	Class Name	Description
1	Unclassified	Processed, but not classified
2	Ground	Bare earth
W7	Low Point (Noise)	Spurious low point returns. Withheld bit set
9	Water	Water surface returns from topographic laser
17	Bridge Deck	Bridges
W18	High Noise	Spurious high point returns. Withheld bit set
20	Ignored Ground	Breakline proximity
40	Bathymetric Point	Submerged topography
41	Water Surface	Water surface returns from bathymetric laser
S42	Derived Water Surface	Synthetic water surface returns used in computing refraction at water surface. Synthetic bit set.
43	Submerged Object	Submerged Object (e.g. wreck, submerged piling)
W45	No Bottom At	Neither surface nor bottom. Withheld bit set.

APPENDIX A : FLIGHT LOGS

APPENDIX B : PROCESSING LOGS